Formation and fragmentation of unsaturated fatty acid $[M - 2H + Na]^-$ ions: Stabilized carbanions for charge-directed fragmentation

Michael C. Thomas[1*], Benjamin B. Kirk[2], Jens Altvater[1], Stephen J. Blanksby[2] and Geoffrey W. Nette[1]

[1] Independent Marine Biochemistry Research, Moreton Bay Research Station, Dunwich, Qld 4183, Australia

[2] ARC Centre of Excellence for Free Radical Chemistry and Biotechnology, School of Chemistry, University of Wollongong, Wollongong, NSW 2522, Australia

[*] Address reprint requests to Dr. Michael C. Thomas, Independent Marine Biochemistry Research, Moreton Bay Research Station, Dunwich, Qld 4183, Australia. E-mail: Michaelt293@gmail.com

Abstract

Fatty acids are long-chain carboxylic acids that readily produce $[M - H]^-$ ions upon negative ion electrospray ionization (ESI) and *cationic* complexes with alkali, alkaline earth and transition metals in positive ion ESI. In contrast, only one *anionic* monomeric fatty acid-metal ion complex has been reported in the literature, namely $[M - 2H + Fe^{II}Cl]^-$. In this manuscript, we present two methods to form *anionic* unsaturated fatty acid-sodium ion complexes, *i.e.*, $[M - 2H + Na]^-$. We find that these ions may be generated efficiently by two distinct methods: (i) Negative ion ESI of a methanolic solution containing the fatty acid and sodium fluoride forming an $[M - H + NaF]^-$ ion. Subsequent collision-induced dissociation (CID) results in the desired $[M - 2H + Na]^-$ ion via the neutral loss of HF. (ii) Direct formation of the $[M - 2H + Na]^-$ ion by negative ion ESI of a methanolic solution containing the fatty acid and sodium hydroxide or bicarbonate. In addition to deprotonation of the carboxylic acid moiety, formation of $[M - 2H + Na]^-$ ions requires the removal of a proton from the fatty acid acyl chain. We propose that this deprotonation occurs at the *bis*-allylic position(s) of polyunsaturated fatty acids resulting in the formation of a resonance-stabilized carbanion. This proposal is supported by *ab initio* calculations which reveal that removal of a proton from the *bis*-allylic position, followed by neutral loss of HX (where $X = F^-$ and ^-OH), is the lowest energy dissociation pathway.

Introduction

Fatty acids are an important structural component for the majority of lipid classes [1]. Within phospholipids, the hydrophobic fatty acid acyl chains are crucial in forming biological membranes where they may establish specific interactions with membrane proteins [2, 3]. Furthermore, free polyunsaturated fatty acids, such as arachidonic acid and docosahexaenoic acid, may be converted to oxygenated derivatives known as eicosanoids and docosanoids which exert potent biological effects [4, 5].

Routine analysis of fatty acids typically involves performing gas chromatography-mass spectrometry (GC-MS) on fatty acid methyl esters using electron ionization (EI) [6]; however, it is also possible to directly ionize underivatized fatty acids by EI to form radical cations ($[M]^{\bullet+}$) [7]. Conversely, when underivatized fatty acids are ionized by either fast-atom bombardment (FAB) or electrospray ionization (ESI), even-electron ions are formed in both negative and positive ion modes. In negative ion FAB and ESI, fatty acids form abundant $[M-H]^-$ ions via the deprotonation of the carboxylic acid functional group [8, 9]. In positive ion mode, abundant fatty acid-metal ion complexes may be generated by cation attachment during ionization in the presence of a metal salt.

A broad range of cationic fatty acid-metal ion complexes have been formed by both FAB and ESI including alkali [10-13], alkaline earth [14, 15] and transition [16, 17] metal ion complexes. Cationic fatty acid-alkali metal ion complexes were first studied by Adams and Gross using FAB. Both $[M + Cat]^+$ and $[M - H + 2Cat]^+$ ions, where Cat = Li^+, Na^+, K^+, Rb^+ and Cs^+, were observed when the FAB matrix was saturated with either an alkali metal iodide or hydroxide [10]. Of these ions, $[M - H + 2Li]^+$ ions have proven particularly useful in determining double bond position by both low and high-energy collision-induced dissociation

(CID) after formation by ESI or matrix-assisted laser desorption ionization (MALDI) [11, 12, 18]. Using ESI, $[M - H + 2Li]^+$ ions have been formed from solutions containing the fatty acid and either lithium acetate or hydroxide [11, 12]. Alternatively, Trimpin *et al.* demonstrated that $[M - H + 2Li]^+$ ions can be formed efficiently using solvent-free MALDI with LiCl and 7,7,8,8-tetracyanoquinodimethane as the matrix [18].

An analogy between the mass spectrometric analysis of fatty acids and small peptides may be made. While small peptides are commonly ionized as $[M + H]^+$ ions due to the presence of basic functional groups [19], peptides also possess a carboxylic acid functional group at the C-terminus and may therefore be ionized in negative ion mode as $[M - H]^-$ ions [20]. Furthermore, cationic peptide-metal ion complexes have been studied in detail as a possible means to provide complementary information for peptide sequencing [21]. Unlike fatty acids, however, anionic peptide-metal ion complexes have also been investigated with alkali [22, 23], alkaline earth [24-27] and transition metals [28-30].

To the authors' knowledge, only one report of an anionic monomeric fatty acid-metal ion complex exists in the literature. In this report, Budimir and co-workers acquired a post-source decay spectrum for a ferric cationized saturated fatty acid heterodimer, $[(M - H) + (M' - H) + Fe^{II}Cl]^-$, and observed $[M - 2H + Fe^{II}Cl]^-$ ions for both fatty acids [31]. In this manuscript we present two methods for the formation of anionic unsaturated fatty acid-sodium ion complexes ($[M - 2H + Na]^-$), rationale for their formation and a discussion of their structure. Subjecting $[M - 2H + Na]^-$ ions to CID results in extensive fragmentation of the fatty acid acyl chain. A comprehensive examination of the dissociation behaviors of these ions will be discussed in a future publication.

Materials and Methods

Materials and sample preparation

Fatty acid standards were purchased from Cayman Chemical (Ann Arbor, MI, USA) via the Australian distributor Sapphire Bioscience (Waterloo, NSW, Australia) and include octadecanoic acid (18:0), 9*Z*-octadecenoic acid (18:1), 9*Z*,12*Z*-octadecadienoic acid (18:2), 8*Z*,11*Z*,14*Z*-eicosatrienoic acid (20:3), 5*Z*,8*Z*,11*Z*,14*Z*-eicosatetraenoic acid (20:4), 5*Z*,8*Z*,11*Z*,14*Z*,17*Z*-eicosapentaenoic acid (20:5) and 4*Z*,7*Z*,10*Z*,13*Z*,16*Z*,19*Z*-docosahexaenoic acid (22:6). LC-MS grade methanol (B&J Brand, Honeywell) was used for sample preparation and HPLC instrument operation. Deionized water was obtained from a Milli-Q Plus filtration system (Millipore, Billerica, MA, USA). Sodium fluoride, sodium chloride, sodium acetate trihydrate and sodium bicarbonate were purchased from Sigma-Aldrich (St Louis, MO, USA) and sodium hydroxide was obtained from APS Chemicals (Seven Hills, NSW, Australia). Nitrogen for operation of the mass spectrometer was sourced using a Domnick Hunter LCMS30-1-E nitrogen generator (Parker Hannifin Ltd., England).

Sodium salt (1 mM NaX; where X = F^-, Cl^- and OAc^-) stock solutions were prepared using deionized water. For CID experiments of fatty acid $[M - H + NaX]^-$ ions, fatty acid solutions were made to a concentration of 1 ng/μL (approx. 3-4 μM) with 100 μM NaX in methanol/water/acetonitrile (89:10:1 by volume). For experiments on the direct formation of fatty acid $[M - 2H + Na]^-$ ions during ESI, solutions of 1 ng/μL 22:6 with 200 μM NaOH and $NaHCO_3$ in methanol/water/acetonitrile (79:20:1 by volume) were prepared. In the control experiment (Figure 3c), a solution of 1 ng/μL 22:6 in methanol/water/acetonitrile (79:20:1 by volume) was prepared without the addition of a sodium salt. To test for the formation of methoxide during ESI, solutions of methanol/water (4:1 v/v), methanol/water (4:1 v/v) with 200 μM NaOH and methanol/water (4:1 v/v) with 200 μM $NaHCO_3$ were prepared.

Mass spectrometry

For $[M - H + NaX]^-$ ion CID experiments, an Agilent 1200 Series HPLC instrument (Waldbronn, Germany) was connected to an LTQ XL linear ion-trap mass spectrometer (Thermo Fisher Scientific, San Jose, USA) fitted with an IonMax electrospray ionization source. The 1200 Series HPLC instrument was used without a column installed and had the following components: micro degasser (G1379B); binary pump SL (G1312B); and high-performance autosampler SL (G1367C). Analysis was automated using the Xcalibur software (Thermo Fisher Scientific, San Jose, USA) and was performed as follows: 100 µL of fatty acid-sodium salt solutions were injected using the autosampler while a flow rate of 10 µL/min was maintained by pumping methanol through the B channel. The mass spectrometer was operated in the negative ion mode with the following settings: source voltage -3.2 kV; tube lens -75 V; capillary voltage -13 V; capillary temperature 320˚C; sheath gas 0 (arbitrary units); and auxiliary gas 20 (arbitrary units). "CID energy bracketing" was employed whereby CID spectra were acquired using integral normalized collision energies from 20 to 25% with an isolation width of 1 Th. In the event that a normalized collision energy of 25% did not provide adequate fragmentation of the precursor ion (precursor ion relative abundance > 50%), the process was repeated with normalized collision energies of 26 to 31%. For CID spectra (or data derived therefrom) presented within this paper, collision energies providing precursor ion relative abundances of between 1 and 28% were selected in post-processing. Prior to acquiring CID spectra, ESI mass spectra were also acquired for all fatty acid-sodium salt solutions analyzed. To acquire a CID spectrum for the $[M - 2H + Na]^-$ ion of 22:6 in an MS^3 experiment, the $[M - H+NaF]^-$ ion was fragmented (collision energy of 25%) and the $[M - 2H + Na]^-$ ion at *m/z* 349 was subsequently fragmented using a collision energy of 24%.

For experiments on the direct formation of $[M - 2H + Na]^-$ ions, ESI mass spectra were recorded while solutions were directly infused at a flow rate of 3 μL/min. ESI-MS parameters utilized were: source voltage -2.5 kV; tube lens -75 V; capillary voltage -28.5 V; capillary temperature 320˚C; sheath gas 35 (arbitrary units); auxiliary gas 36 (arbitrary units); and sheath gas 10 (arbitrary units). A CID spectrum for the $[M - H + Na]^-$ ion of 22:6, produced from the methanolic solution containing sodium hydroxide, was acquired using a collision energy of 24%. To test for the formation of methoxide, ESI mass spectra were acquired from *m/z* 15 to 70 over a 1 min time period while solutions were directly infused at a flow rate of 5 μL/min. Instrument settings used were: source voltage -2.7 kV; tube lens -42.5 V; capillary voltage -44 V; capillary temperature 275˚C; sheath gas 11 (arbitrary units); auxiliary gas 0 (arbitrary units); and sheath gas 1 (arbitrary units).

Computational chemistry

All calculations were undertaken using the density functional theory M06-2X method [32] and the 6-31+G(d) basis set within the GAUSSIAN09 suite of programs [33]. All stationary points calculated in this manuscript were characterized as minima (no imaginary frequencies). Calculated energies include unscaled zero-point energies at the same level. Complete geometries and calculated energies are available in Supplementary Material.

Results and Discussion

Formation of $[M - 2H + Na]^-$ ions by CID of fatty acid-sodium fluoride complexes

The negative ion ESI mass spectrum of a methanolic solution of 3 μM 20:3 with 100 μM sodium fluoride is shown in Figure 1(a). In this spectrum, an abundant ion at *m/z* 305 is observed and is the deprotonated ion, $[M - H]^-$, of 20:3. In addition, a less abundant ion at *m/z* 347 is also observed and is assigned as the fatty acid-sodium fluoride complex, [M - H +

NaF]$^-$, resulting from the addition of NaF to the electrospray solvent. A CID spectrum of the [M - H + NaF]$^-$ ion was acquired and displays two major product ions at *m/z* 305 and 327 (Figure 1b). The peak at *m/z* 305 corresponds to the [M - H]$^-$ ion of 20:3 (as observed in Figure 1a) and is formed by neutral loss of NaF from the [M - H + NaF]$^-$ precursor ion. Conversely, the base peak at *m/z* 327 represents a neutral loss of 20 Da corresponding to the loss of HF. Intriguingly, this implies that deprotonation of the fatty acyl chain occurs to form a [M - 2H + Na]$^-$ ion at *m/z* 327.

The CID spectra for the [M - H + NaF]$^-$ ions of the fully saturated 18:0 and polyunsaturated 22:6 fatty acids are shown in Figures 2(a) and (b). For 18:0, the base peak at *m/z* 283 corresponds to the [M - H]$^-$ ion and the [M - 2H + Na]$^-$ ion expected at *m/z* 305 is of exceedingly low abundance (Figure 2a). For 22:6, the opposite is observed, where the [M - 2H + Na]$^-$ ion at *m/z* 349 is the base peak and the [M - H]$^-$ ion at *m/z* 327 is of low abundance (Figure 2b). A CID spectrum acquired in the MS^3 mode for the [M - 2H + Na]$^-$ ion of 22:6 is provided in Figure 2(c). This CID spectrum displays richer fragmentation chemistry than observed from CID of the conventional [M - H]$^-$ ion of 22:6, which predominately loses carbon dioxide when subjected to CID [34]. Product ions arising from cleavages along the acyl chain are observed in the CID spectrum for the [M - 2H + Na]$^-$ ion of 22:6; these include ions of *m/z* 121, 135, 161, 175, 187, 201, 215, 227, 241 and 279. In addition, consecutive neutral losses of 2 Da, corresponding to H_2, are also observed with product ions at *m/z* 347, 345, 343 and 341. (Figure 2c). The majority of these product ions arising from H_2 neutral losses and acyl chain cleavages are also observed at low abundance in the CID spectrum for the [M - H + NaF]$^-$ ion of 22:6 (Figure 2b), suggesting that these ions arise from secondary fragmentation of the [M - 2H + Na]$^-$ product ion at *m/z* 349. Moreover, an *m/z* 283 product

ion is also observed in Figure 2(b) and likely arises from secondary fragmentation of the [M - H]$^-$ product ion at *m/z* 327 [34].

A product ion at *m/z* 183 is observed with a relative abundance of 32% in the CID spectrum for the [M - H + NaF]$^-$ ion of 18:0 (Figure 2a). This is unexpected and cannot be rationalized as secondary fragmentation of 18:0 as saturated carboxylate anions eliminate water upon CID [35]. It was hypothesized that the *m/z* 183 product ion originates from an isobaric contaminant. During our experiments, contaminant ions were commonly observed at *m/z* 311, 325 and 339; where the *m/z* 325 contaminant ion is isobaric with the [M - H + NaF]$^-$ ion of 18:0. CID was performed on *m/z* 325 contaminant ion and an abundant product ion was observed at *m/z* 183 (Figure S1(a), Supplementary Material), thereby supporting the initial hypothesis. This fragmentation is consistent with C_{12} linear alkylbenzene sulfonates where the *m/z* 183 product ion has the proposed structure of 4-vinylbenzenesulfonate [36]. This structural assignment of the *m/z* 325 contaminant ion is also supported by high-resolution MS on a Bruker micrOTOF-Q which revealed an elemental composition of $C_{18}H_{29}O_3S$ (measured *m/z* 325.1843; expected *m/z* 325.18374). MS^3 CID spectra were also acquired for the *m/z* 183 product ions from the *m/z* 325 contaminant ion and [M - H + NaF]$^-$ ion of 18:0 (see Figure S1(b and c), Supplementary Material). These MS^3 CID spectra are essentially identical with abundant *m/z* 119 product ions observed in both cases. The *m/z* 119 ions represent neutral losses of 64 Da, corresponding to the loss of SO_2, which is characteristic of aromatic sulfonate anions [37]. These data therefore provide conclusive evidence that the *m/z* 183 ion originates from isobaric C_{12} linear alkylbenzene sulfonates and not from the 18:0 [M - H + NaF]$^-$ precursor ion.

The possibility that fluoride at *m/z* 19 is also a CID product for the $[M - H + NaF]^-$ ions of 18:0, 20:3 and 22:6 was considered. The fluoride anion is below the low-mass cutoff of the ion-trap mass spectrometer used in these experiments and therefore cannot be observed in Figures 1(b), 2(a) and 2(b), even if it were a CID product ion. However, a substantial decrease in total ion current was not observed with the onset of $[M - H + NaF]^-$ ion fragmentation (data not shown), thus suggesting fluoride formation is not a major dissociation channel. Nevertheless, the possibility that fluoride is formed in low abundances cannot be excluded.

Effect of degree of unsaturation on $[M - 2H + Na]^-$ ion formation

To investigate the effect of degree of unsaturation, CID was also performed on the $[M - H + NaF]^-$ ions of 18:1, 18:2, 20:4 and 20:5 (Table 1). For these fatty acid-sodium fluoride complexes, the $[M - H]^-$ and $[M - 2H + Na]^-$ ions were the main CID products (Equations 1-2), with only minor secondary fragmentation or competing primary pathways observed (Table 1).

$$[M - H + NaF]^- \rightarrow [M - H]^- + NaF \quad (1)$$

$$\rightarrow [M - 2H + Na]^- + HF \quad (2)$$

Abundances for the $[M - 2H + Na]^-$ product ion (normalized to total product ion abundance) and $[M - 2H + Na]^-/[M - H]^-$ branching ratios were calculated for fatty acid-sodium fluoride complexes of 18:0, 18:1, 18:2, 20:3, 20:4, 20:5 and 22:6 (Table 2). A general trend of increasing $[M - 2H + Na]^-$ ion abundance and $[M - 2H + Na]^-/[M - H]^-$ branching ratio is observed with increasing degrees of unsaturation. The $[M - 2H + Na]^-$ ion abundances and $[M - 2H+ Na]^-/[M - H]^-$ branching ratios are very low for the saturated 18:0 and monounsaturated

18:1 (abundances of 0.031% and 0.064%, respectively; $[M - 2H + Na]^-/[M - H]^-$ branching ratios of $4.7x10^{-4}$ and $6.4x10^{-4}$, respectively). Significantly, however, a marked increase in the $[M - 2H + Na]^-$ ion abundance and $[M - 2H + Na]^-/[M - H]^-$ branching ratio is observed for 18:2 (39.7% and $6.7x10^{-1}$, respectively). The trend of increasing $[M - 2H + Na]^-$ ion abundance and $[M - 2H + Na]^-/[M - H]^-$ branching ratio continues to 22:6 (87.5% and 46.4, respectively).

Mechanism for the formation of $[M - 2H + Na]^-$ ions

The polyunsaturated fatty acids studied here are all methylene interrupted and thus contain at least one *bis*-allylic position. The *ca.* 620 fold increase in $[M - 2H + Na]^-$ product ion abundance and *ca.* 1000 fold increase in $[M - 2H + Na]^-/[M - H]^-$ branching ratio when going from 18:1 (two *mono*-allylic positions) to 18:2 (two *mono*-allylic positions and one *bis*-allylic position) strongly suggests that at least one *bis*-allylic position is required for the facile formation of an abundant $[M - 2H + Na]^-$ ion. Therefore, we propose a mechanism whereby proton transfer from a *bis*-allylic position to the fluoride anion occurs resulting in the neutral loss of HF and formation of a resonance-stabilized carbanion (Scheme 1). For fatty acids with three or more double bonds, multiple *bis*-allylic positions are available for deprotonation. For example, deprotonation may occur at either C10 or C13 for 20:3 (Scheme 1). This suggests the possibility of two isomeric $[M - 2H + Na]^-$ ions for 20:3 differing in the location of the resonance-stabilized carbanion. Of interest, ions of analogous structure to that proposed in Scheme 1 for the fatty acid $[M - 2H + Na]^-$ ion have also been produced by CID of dicarboxylic acid $[M - 2H + Li]^-$ ions, where decarboxylation results in the formation of a carbanion [38]. It should be noted, however, that Scheme 1 does not rationalize the observation of $[M - 2H + Na]^-$ ions for the saturated 18:0 and monounsaturated 18:1 fatty acids which lack a *bis*-allylic position. For these fatty acids, deprotonation has to occur

elsewhere on the fatty acyl chain, such as the α-carbon at C2 or allylic positions of 18:1 at C8 and C11. Although, the very low abundance of the $[M - 2H + Na]^-$ ions for 18:0 and 18:1 suggests that deprotonation at the α-carbon or allylic positions is unfavorable.

Effect of anion type

From the mechanism proposed in Scheme 1, it would be expected that the gas-phase basicity of the adducting anion would affect the branching between the $[M - 2H + Na]^-$ and $[M - H]^-$ fragmentation channels, *i.e.*, the gas-phase basicity should regulate the proton transfer reaction. To test the effect of anion basicity on the formation of fatty acid $[M - 2H + Na]^-$ ions, CID was performed on $[M - H + NaX]^-$ ions of 20:3; where X = F^-, Cl^- and OAc^-. In addition, CID was also performed on the sodium-bound homodimer of 20:3 observed in the ESI mass spectrum of 20:3 with NaF. Abundances of the $[M - 2H + Na]^-$ ion (normalized to total product ion abundance) and $[M - 2H + Na]^-/[M - H]^-$ branching ratios for these complexes are presented in Table 3. For the 20:3-sodium fluoride complex, the $[M - 2H + Na]^-$ ion abundance and $[M - 2H + Na]^-/[M - H]^-$ branching ratio are 79.5% and 4.1, respectively. In comparison, the $[M - 2H + Na]^-$ ions generated from the sodium chloride and sodium acetate complexes are of very low abundance (0.047% and 0.17%, respectively), *i.e.*, formation of the $[M - H]^-$ product ion is the favored dissociation pathway. In addition, the abundance of the $[M - 2H + Na]^-$ ion formed from the sodium-bound homodimer is close to that of the $[M - H + NaOAc]^-$ ion at 0.19% (Table 3).

The ability of the anion to deprotonate a *bis*-allylic position of 20:3 may be summarized as follows: $F^- >> OAc^- > Cl^-$. This aligns with the order of experimental gas-phase basicities: F^- = 1530 kJ/mol [39, 40]; OAc^- = 1429 kJ/mol [39, 41]; and Cl^- = 1373 kJ/mol [39, 42]. The $[M - 2H + Na]^-$ ion of 20:3 was the base peak only for the fatty acid-sodium fluoride complex

suggesting its gas-phase basicity lies between that of fluoride and acetate, *i.e.*, 1429-1530 kJ/mol.

Direct formation of [M - 2H + Na]$^-$ anions by electrospray ionization

The ESI mass spectrum of a methanolic solution of 3 μM 22:6 with 200 μM NaOH is shown in Figure 3(a). A peak at *m/z* 327 is observed corresponding to the [M - H]$^-$ ion of 22:6. Interestingly, however, an [M - H + NaOH]$^-$ ion at *m/z* 367 was not observed (data not shown). Instead, an ion at *m/z* 349 is observed with a relative abundance of 8.1%, representing the [M - 2H + Na]$^-$ ion of 22:6 (Figure 3a). When 200 μM $NaHCO_3$ was used in place of 200 μM NaOH, the resulting ESI mass spectrum is essentially the same, with the appearance of the [M - 2H + Na]$^-$ ion at *m/z* 349 (relative abundance of 8.1% - Figure 3b) and the absence of an [M - H + $NaHCO_3$]$^-$ ion at *m/z* 411. A CID spectrum of the [M - 2H + Na]$^-$ ion at *m/z* 349 formed by the ESI of 22:6 with NaOH is shown in Figure 3(d). This spectrum displays the same product ions as observed in the CID spectrum for the [M - 2H + Na]$^-$ product ion from the sodium fluoride complex of 22:6 (Figure 2c), thereby confirming that the *m/z* 349 ion is indeed the 22:6 [M - 2H + Na]$^-$ ion. The CID spectra of the [M - 2H + Na]$^-$ ions formed via the two different methods are not identical. Significantly, the CID spectrum of the [M - 2H + Na]$^-$ ion formed directly by ESI of 22:6 with NaOH displays product ions originating from acyl chain cleavages in higher abundances. The differences between these two CID spectra provide further evidence against deprotonation at the α-position since if deprotonation occurred exclusively at the α-position in both methods, the CID spectra should be identical. Conversely, the differences between the two CID spectra can be rationalized by different distributions of the five possible isomeric ions for 22:6 when deprotonation occurs at the *bis*-allylic positions. The acyl chain cleavages observed in Figures 2(c) and 3(d) provide information on double bond position and likely occur by charge-driven fragmentation

mechanisms at the site of the resonance-stabilized carbanion (see Scheme S1, Supplementary Material, for a proposed mechanism for the *m/z* 215 product ion). A full investigation of these fragmentation mechanisms is, however, beyond the scope of this study.

A control experiment was also performed, whereby a 3 μM 22:6 solution with no added sodium salt was ionized under identical conditions (Figure 3c). In this spectrum, an ion of *m/z* 349 was observed with a relative abundance of 1.6%. CID was performed on the *m/z* 349 ion observed in Figure 3(c) and confirmed at least a minor contribution of the 22:6 $[M - 2H + Na]^-$ ion to the *m/z* 349 ion population (data not shown). This suggests that anionic fatty acid-sodium ion complexes can be formed from background sodium under favorable ionization conditions.

Cai and Cole have previously demonstrated that the stability of anionic adducts is controlled by the relative gas-phase basicities of the deprotonated analyte molecule, $[M - H]^-$, and the adducting anion [43]. The complex formed between the analyte molecule and adducting anion is most stable when the gas-phase basicities of the deprotonated analyte molecule and adducting anion are similar [43]. A modification of this principle is required when considering fatty acid $[M - H + NaX]^-$ complexes. That is, it may be expected that the direct loss of HX will occur if the gas-phase basicity of the adducting anion, X^-, is much greater than that of the $[M - 2H + Na]^-$ ion. The gas-phase basicity of hydroxide is 1606 kJ/mol [39, 44], which is higher than that of fluoride. Therefore, it is proposed that the higher gas-phase basicity of hydroxide means that a stable fatty acid-sodium hydroxide complex cannot be formed as it will dissociate to form the $[M - 2H + Na]^-$ ion. This does not, however, explain the absence of an $[M - H + NaHCO_3]^-$ ion and appearance of the $[M - 2H + Na]^-$ ion in the ESI mass spectrum of 22:6 with $NaHCO_3$ (Figure 3b). Bicarbonate has a gas-phase basicity

of 1458 kJ/mol [45] which is less than the gas-phase basicity of fluoride and closer to that of acetate. Based on gas-phase basicities, it may therefore be expected that a stable [M - H + $NaHCO_3$]$^-$ ion should be observed in the ESI mass spectrum of 22:6 with $NaHCO_3$. Indeed, anionic steroid-bicarbonate complexes have previously been observed [46, 47], further suggesting that the [M - H + $NaHCO_3$]$^-$ ion should be observed in the ESI mass spectrum of 22:6 with $NaHCO_3$.

To rationalize the absence of the [M - H + $NaHCO_3$]$^-$ ion, it was hypothesized that methoxide is formed during the ionization process via a reaction between methanol, the electrospray solvent, and bicarbonate. The gas-phase basicity of the methoxide anion is 1573 kJ/mol [39, 48, 49] which is higher than that of fluoride. This would account for the [M - 2H + Na]$^-$ ion observed in Figure 3(b) since dissociation of the fatty acid-sodium methoxide complex may be expected during the electrospray process. In fact, the higher gas-phase basicity of hydroxide may even suggest that methoxide, and not hydroxide, drives the formation of the [M - 2H + Na]$^-$ ion in the ESI mass spectrum of 22:6 with NaOH (Figure 3a). To examine this hypothesis, ESI mass spectra were acquired from *m/z* 15 to 70 for the following solutions: methanol/water (4:1 v/v); methanol/water (4:1 v/v) with 200 μM NaOH; methanol/water (4:1 v/v) with 200 μM $NaHCO_3$; and methanol/water (4:1 v/v) with 200 μM NaF (data presented in Table 4). Significantly, a ~100 fold increase in the *m/z* 31 ion abundance was observed in the ESI mass spectra of NaOH and $NaHCO_3$ solutions when compared to the ESI mass spectrum of the control solution with no added sodium salt. Moreover, abundant hydroxide and bicarbonate ions were not observed for the NaOH and $NaHCO_3$ solutions whereas an abundant *m/z* 19 ion, corresponding to fluoride, was observed in the ESI mass spectrum of the NaF solution (Table 4). While care must be taken when examining ion abundances in the low-mass region of ion-trap mass spectrometers, the ~100

fold increase in methoxide abundance and absence of abundant hydroxide and bicarbonate ions for the NaOH and $NaHCO_3$ solutions support the hypothesis that $[M-2H+Na]^-$ ion formation is driven by methoxide.

Interestingly, the deprotonation of methanol would not be expected on the basis of basicity in either the condensed or gas phase. However, the drying of negatively-charged droplets formed by ESI results in rapid increases in pH, ion concentration and relative surface area. Under analogous conditions, the rates of bimolecular reactions involving anionic intermediates have been found to increase by up to several orders of magnitude [50]. In addition, bicarbonate exists in equilibrium with carbonic acid and carbon dioxide; furthermore, carbonic acid is not stable in the gas-phase and readily dissociates to form water and carbon dioxide [51]. Considering the changes that occur in negatively-charged droplets and the chemistry of bicarbonate, it is proposed that loss of carbon dioxide from drying charged droplets during the ESI process drives the equilibrium towards the formation of methoxide as shown in Equation 3.

$$HCO_3^-{}_{(aq)} + CH_3OH_{(aq)} \rightarrow CH_3O^-{}_{(g)} + H_2O_{(g)} + CO_{2(g)} \quad (3)$$

Computational chemistry

Ab initio calculations were performed to gain greater insight into the stability and dissociation of $[M - H + NaX]^-$ complexes. As a model system, the deprotonated fatty acid, 4*Z*,7*Z*-nonadienoate (9:2), was complexed with sodium fluoride and sodium hydroxide. Potential energy diagrams for the formation and dissociation of these complexes are provided in Figures 4(a) and (b).

Complexing NaF to the $[M - H]^-$ ion of 9:2 is exothermic by 53.3 kcal/mol (Figure 4a). Several local minima were identified for the $[M - H + NaF]^-$ ion where the sodium cation is situated between the carboxylate and fluoride anions. In the lowest energy structure, additional stability is gained through interactions between fluoride and the partial positive charges of allylic hydrogens (Figure 4a). All structures for the $[M - H + NaF]^-$ ion return energies within 4 kcal/mol suggesting that many different structures may be sampled over the lifetime of a vibrationally-activated species. Three possible dissociation channels for the $[M - H + NaF]^-$ ion of 9:2 were considered, these are $[M - 2H + Na]^-$, $[M - H]^-$ and F^- ion formation. In the case of $[M - 2H + Na]^-$ ion formation, three sites of deprotonation were considered: (i) the *bis*-allylic position at C6; (ii) the *mono*-allylic position at C9; and (iii) the α-position at C2. The lowest energy dissociation pathway is $[M - 2H + Na]^-$ ion formation where fluoride deprotonates the *bis*-allylic position at C6 (endothermic by 41.1 kcal/mol – note that an ion-dipole complex was not identified between HF and the $[M - 2H + Na]^-$ ion). The structure of the $[M - 2H + Na]^-$ ion from this pathway is shown in Figure 4 and has the sodium cation bridging the carboxylate and resonance-stabilized carbanion. In contrast, deprotonation of the *mono*-allylic position at C9 and α-position at C2 are higher energy pathways (endothermic by 53.9 and 85.9 kcal/mol, respectively), supporting the proposed mechanism where deprotonation occurs at a *bis*-allylic position (Scheme 1). The formation of the $[M - H]^-$ ion is the reverse process to the formation of the fatty acid-sodium fluoride complex and is thus endothermic by 53.3 kcal/mol. F^- ion formation via the neutral loss of the fatty acid sodium salt is a higher energy pathway than $[M - H]^-$ ion formation and $[M - 2H + Na]^-$ ion formation when deprotonation occurs at the *bis*-allylic position (endothermic by 59.0 kcal/mol). This is consistent with the earlier assertion that F^- ion formation is at most a minor dissociation channel. For the 18:2 fatty acid, the $[M - H]^-$ ion was the major CID product from the $[M - H + NaF]^-$ complex (Table 1). In contrast, these calculations reveal that [M -

2H + Na]$^-$ ion formation is the lowest energy dissociation channel for the 9:2-sodium fluoride complex. This apparent discrepancy may be attributed to differences between the model system and 18:2 fatty acid. More likely, however, is the possibility that NaF neutral loss is entropically favored over HF neutral loss where the fluoride anion has to align with a *bis*-allylic hydrogen within the [M - H + NaF]$^-$ complex.

The potential energy diagram for the 9:2-sodium hydroxide complex (Figure 4b) differs greatly from that of the sodium fluoride complex (Figure 4a). Significantly, proton transfer from the *bis*-allylic position to hydroxide within the [M - H + NaOH]$^-$ complex is exothermic by 0.4 kcal/mol. This results in the formation of a stable [M - 2H + Na + H_2O]$^-$ complex. Neutral loss of H_2O from this complex to form the [M - 2H + Na]$^-$ ion is then endothermic by 17.3 kcal/mol. The formation of [M - H]$^-$ and $^-$OH ions are much higher energy processes (endothermic by 47.2 kcal/mol and 56.9 kcal/mol, respectively). The comparatively low energy to form the [M - 2H + Na]$^-$ ion suggests that excitation could conceivably be achieved during the ion generation and isolation process. These data therefore provide mechanistic insight into the direct formation of [M - 2H + Na]$^-$ ions by strongly basic anions during the electrospray process (*i.e.*, hydroxide and methoxide).

Conclusion

We have demonstrated that fatty acid [M - 2H + Na]$^-$ ions may be formed efficiently via two methods: (i) CID of fatty acid [M - H + NaF]$^-$ complexes; and (ii) direct formation by electrospray ionization of the fatty acid in the presence of sodium hydroxide or bicarbonate. The formation of [M - 2H + Na]$^-$ ions is not without precedent as peptide [M - 2H + Na]$^-$ ions [22, 23] and fatty acid [M - 2H + $Fe^{II}Cl$]$^-$ ions [31] have previously been reported. However, the formation of peptide [M - 2H + Na]$^-$ ions requires the deprotonation of an amide nitrogen

[22, 23] whereas a carbanion is formed for fatty acid $[M - 2H + Na]^-$ ions. Moreover, deprotonation occurs at the *bis*-allylic positions of polyunsaturated fatty acids in the formation of $[M - 2H + Na]^-$ ions. This differs from saturated fatty acid $[M - 2H + Fe^{II}Cl]^-$ ions, where deprotonation was proposed to occur at the α-position [31]. The two methods for $[M - 2H + Na]^-$ ion formation allow the CID of these ions to be investigated for the first time. The presence of a carbanion on the fatty acyl chain suggests that charge-driven fragmentation processes occur in the CID of fatty acid $[M - 2H + Na]^-$ ions resulting in abundant product ions from acyl chain cleavages. The nature of these fragmentation mechanisms and their pertinence for structural characterization are the subject of ongoing investigations.

Acknowledgements

M.C.T., J.A. and G.W.N. would like to acknowledge Moreton Bay Research Station (MBRS) for providing laboratory space and Graham MacFarlane (University of Queensland) for providing high-resolution mass spectrometry data. S.J.B. and B.B.K. acknowledge funding through the Australian Research Council (ARC) Centre of Excellence for Free Radical Chemistry and Biotechnology (CE0561607) and an ARC Discovery grant (DP120102922). B.B.K. and S.J.B. are grateful to the NCI National Facility for a generous allocation of computing time through the Merit Allocation Scheme. M.C.T. would like to acknowledge Thomas Gallagher (IMBCR) for laboratory assistance, Richard Moxham for assistance in preparing the manuscript and Dr. Mei Bai (University of Melbourne) for helpful discussions and support.

References

1. Fahy, E.; Subramaniam, S.; Brown, H. A.; Glass, C. K.; Merrill, A. H.; Murphy, R. C.; Raetz, C. R. H.; Russell, D. W.; Seyama, Y.; Shaw, W.; Shimizu, T.; Spener, F.; van Meer, G.; VanNieuwenhze, M. S.; White, S. H.; Witztum, J. L., and Dennis, E. A. A comprehensive classification system for lipids. Journal of Lipid Research, 2005. 46(5), 839-861.
2. Shinzawa-Itoh, K.; Aoyama, H.; Muramoto, K.; Terada, H.; Kurauchi, T.; Tadehara, Y.; Yamasaki, A.; Sugimura, T.; Kurono, S.; Tsujimoto, K.; Mizushima, T.; Yamashita, E.; Tsukihara, T., and Yoshikawa, S. Structures and physiological roles of 13 integral lipids of bovine heart cytochrome c oxidase. Embo Journal, 2007. 26(6), 1713-1725.
3. Brown, S. H. J.; Mitchell, T. W.; Oakley, A. J.; Pham, H. T., and Blanksby, S. J. Time to face the fats: What can mass spectrometry reveal about the structure of lipids and their interactions with proteins? Journal of the American Society for Mass Spectrometry, 2012. 23(9), 1441-1449.
4. Tapiero, H.; Ba, G. N.; Couvreur, P., and Tew, K. D. Polyunsaturated fatty acids (PUFA) and eicosanoids in human health and pathologies. Biomedicine & Pharmacotherapy, 2002. 56(5), 215-222.
5. Serhan, C. N. Novel eicosanoid and docosanoid mediators: resolvins, docosatrienes, and neuroprotectins. Current Opinion in Clinical Nutrition and Metabolic Care, 2005. 8(2), 115-121.
6. Eder, K. Gas chromatographic analysis of fatty acid methyl esters Journal of Chromatography B-Biomedical Applications, 1995. 671(1-2), 113-131.
7. Trufelli, H.; Famiglini, G.; Termopoli, V., and Cappiello, A. Profiling of non-esterified fatty acids in human plasma using liquid chromatography-electron

ionization mass spectrometry. Analytical and Bioanalytical Chemistry, 2011. 400(9), 2933-2941.

8. Tomer, K. B.; Crow, F. W., and Gross, M. L. Location of double-bond position in unsaturated fatty acids by negative ion MS/MS. Journal of the American Chemical Society, 1983. 105(16), 5487-5488.

9. Kerwin, J. L.; Wiens, A. M., and Ericsson, L. H. Identification of fatty acids by electrospray mass spectrometry and tandem mass spectrometry. Journal of Mass Spectrometry, 1996. 31(2), 184-192.

10. Adams, J. and Gross, M. L. Tandem mass spectrometry for collisional activation of alkali metal-cationized fatty acids: a method for determining double bond location. Analytical Chemistry, 1987. 59(11), 1576-1582.

11. Hsu, F. F. and Turk, J. Distinction among isomeric unsaturated fatty acids as lithiated adducts by electrospray ionization mass spectrometry using low energy collisionally activated dissociation on a triple stage quadrupole instrument. Journal of the American Society for Mass Spectrometry, 1999. 10(7), 600-612.

12. Hsu, F. F. and Turk, J. Elucidation of the double-bond position of long-chain unsaturated fatty acids by multiple-stage linear ion-trap mass spectrometry with electrospray ionization. Journal of the American Society for Mass Spectrometry, 2008. 19(11), 1673-1680.

13. Poad, B. L. J.; Pham, H. T.; Thomas, M. C.; Nealon, J. R.; Campbell, J. L.; Mitchell, T. W., and Blanksby, S. J. Ozone-induced dissociation on a modified tandem linear ion-trap: Observations of different reactivity for isomeric lipids. Journal of the American Society for Mass Spectrometry, 2010. 21(12), 1989-1999.

14. Davoli, E. and Gross, M. L. Charge remote fragmentation of fatty acids cationized with alkaline earth metal ions. Journal of the American Society for Mass Spectrometry, 1990. 1(4), 320-324.

15. Zehethofer, N.; Pinto, D. M., and Volmer, D. A. Plasma free fatty acid profiling in a fish oil human intervention study using ultra-performance liquid chromatography/electrospray ionization tandem mass spectrometry. Rapid Communications in Mass Spectrometry, 2008. 22(13), 2125-2133.

16. Blagojevic, V.; Samad, S. N.; Banu, L.; Thomas, M. C.; Blanksby, S. J., and Bohme, D. K. Mass spectrometric study of the dissociation of Group XI metal complexes with fatty acids and glycerolipids: Ag_2H^+ and Cu_2H^+ ion formation in the presence of a double bond. International Journal of Mass Spectrometry, 2011. 299(2-3), 125-130.

17. Afonso, C.; Riu, A.; Xu, Y.; Fournier, F., and Tabet, J. C. Structural characterization of fatty acids cationized with copper by electrospray ionization mass spectrometry under low-energy collision-induced dissociation. Journal of Mass Spectrometry, 2005. 40(3), 342-349.

18. Trimpin, S.; Clemmer, D. E., and McEwen, C. N. Charge-remote fragmentation of lithiated fatty acids on a TOF-TOF instrument using matrix-ionization. Journal of the American Society for Mass Spectrometry, 2007. 18(11), 1967-1972.

19. Paizs, B. and Suhai, S. Fragmentation pathways of protonated peptides. Mass Spectrometry Reviews, 2005. 24(4), 508-548.

20. Bowie, J. H.; Brinkworth, C. S., and Dua, S. Collision-induced fragmentations of the $(M-H)^-$ parent anions of underivatized peptides: An aid to structure determination and some unusual negative ion cleavages. Mass Spectrometry Reviews, 2002. 21(2), 87-107.

21. Teesch, L. M. and Adams, J. Fragmentations of gas-phase complexes between alkali metal ions and peptides: metal ion binding to carbonyl oxygens and other neutral functional groups. Journal of the American Chemical Society, 1991. 113(3), 812-820.

22. Hu, P. F. and Gross, M. L. Gas-phase anionic complexes of alkali metal ions and peptides: structure and collision activated decompositions. Journal of the American Society for Mass Spectrometry, 1994. 5(3), 137-143.

23. Wang, J. Y.; Ke, F.; Siu, K. W. M., and Guevremont, R. Electrospray tandem mass spectrometry of alkali metal-containing anionic complexes of tripeptide. Journal of Mass Spectrometry, 1996. 31(2), 159-168.

24. Hu, P. F. and Gross, M. L. Strong interactions of anionic peptides and alkaline earth metal ions: metal-ion-bound peptides in the gas phase. Journal of the American Chemical Society, 1992. 114(23), 9153-9160.

25. Hu, P. F. and Gross, M. L. Strong interactions of anionic peptides and alkaline earth metal ions: bis(peptide) complexes in the gas phase. Journal of the American Chemical Society, 1992. 114(23), 9161-9169.

26. Zhao, H.; Reiter, A.; Teesch, L. M., and Adams, J. Gas-phase fragmentations of anionic complexes between peptides and alkaline earth metal ions: structure-specific side-chain interactions. Journal of the American Chemical Society, 1993. 115(7), 2854-2863.

27. Reiter, A.; Teesch, L. M.; Zhao, H., and Adams, J. Gas-phase fragmentations of anionic complexes of serine- and threonine-containing peptides. International Journal of Mass Spectrometry and Ion Processes, 1993. 127, 17-26.

28. Hu, P. F. and Gross, M. L. Gas-phase interactions of transition-metal ions and di- and tripeptides: a comparison with alkaline-earth-metal-ion interactions. Journal of the American Chemical Society, 1993. 115(19), 8821-8828.

29. Bossee, A.; Afonso, C.; Fournier, F.; Tasseau, O.; Pepe, C.; Bellier, B., and Tabet, J. C. Anionic copper complex fragmentations from enkephalins under low-energy collision-induced dissociation in an ion trap mass spectrometer. Journal of Mass Spectrometry, 2004. 39(8), 903-912.

30. Bossee, A.; Fournier, F.; Tasseau, O.; Bellier, B., and Tabet, J. C. Electrospray mass spectrometric study of anionic complexes of enkephalins with Cu(II): regioselective distinction of Leu/Ile at the C-terminus induced by metal reduction. Rapid Communications in Mass Spectrometry, 2003. 17(12), 1229-1239.

31. Budimir, N.; Blais, J. C.; Fournier, F., and Tabet, J. C. Desorption/ionization on porous silicon mass spectrometry (DIOS) of model cationized fatty acids. Journal of Mass Spectrometry, 2007. 42(1), 42-48.

32. Zhao, Y. and Truhlar, D. G. The M06 suite of density functionals for main group thermochemistry, thermochemical kinetics, noncovalent interactions, excited states, and transition elements: two new functionals and systematic testing of four M06-class functionals and 12 other functionals. Theoretical Chemistry Accounts, 2008. 120(1-3), 215-241.

33. Frisch, M. J.; Trucks, G. W.; Schlegel, H. B.; Scuseria, G. E.; Robb, M. A.; Cheeseman, J. R.; Scalmani, G.; Barone, V.; Mennucci, B.; Petersson, G. A.; Nakatsuji, H.; Honda, Y.; Kitao, O.; Nakai, H.; Vreven, T.; Montgomery, J., J. A.; Peralta, J. E.; Ogliaro, F.; Bearpark, M.; Heyd, J. J.; Brothers, E.; Kudin, K. N.; Staroverov, V. N.; Keith, T.; Kobayashi, R.; Normand, J.; Raghavachari, K.; Rendell, A.; Burant, J. C.; Iyengar, S. S.; Tomasi, J.; Cossi, M.; Rega, N.; Millam, J. M.; Klene, M.; Knox, J. E.; Cross, J. B.; Bakken, V.; Adamo, C.; Jaramillo, J.; Gomperts, R.; Stratmann, R. E.; Yazyev, O.; Austin, A. J.; Cammi, R.; Pomelli, C.; Ochterski, J. W.; Martin, R. L.; Morokuma, K.; Zakrzewski, V. G.; Voth, G. A.; Salvador, P.;

Dannenberg, J. J.; Dapprich, S.; Daniels, A. D.; Farkas, O.; Foresman, J. B.; Ortiz, J. V.; Cioslowski, J., and Fox, D. J., Gaussian 09. 2010, Gaussian, Inc.: Wallingford CT.

34. Thomas, M. C.; Dunn, S. R.; Altvater, J.; Dove, S. G., and Nette, G. W. Rapid identification of long-chain polyunsaturated fatty acids in a marine extract by HPLC-MS using data-dependent acquisition. Analytical Chemistry, 2012. 84(14), 5976-5983.

35. Jensen, N. J.; Haas, G. W., and Gross, M. L. Ion—neutral complex intermediate for loss of water from fatty acid carboxylates. Organic Mass Spectrometry, 1992. 27(4), 423-427.

36. Gonzalez-Mazo, E.; Honing, M.; Barcelo, D., and Gomez-Parra, A. Monitoring long-chain intermediate products from the degradation of linear alkylbenzene sulfonates in the marine environment by solid-phase extraction followed by liquid chromatography ionspray mass spectrometry. Environmental Science & Technology, 1997. 31(2), 504-510.

37. Binkley, R. W.; Flechtner, T. W.; Tevesz, M. J. S.; Winnik, W., and Zhong, B. Rearrangement of aromatic sulfonate anions in the gas-phase. Organic Mass Spectrometry, 1993. 28(7), 769-772.

38. Zhang, X. Mass spectrometric and theoretical studies on the decarboxylation of the anionic lithium complexes of the doubly deprotonated dicarboxylic acids. Journal of Molecular Structure, 2012. 1015, 12-19.

39. Bartmess, J. E., "Negative Ion Energetics Data", in NIST Chemistry WebBook, NIST Standard Reference Database Number 69, P.J. Linstrom and W.G. Mallard, Editors, National Institute of Standards and Technology, Gaithersburg MD, 20899, http://webbook.nist.gov, (retrieved January 13, 2013).

40. Blondel, C.; Delsart, C., and Goldfarb, F. Electron spectrometry at the mu eV level and the electron affinities of Si and F. Journal of Physics B-Atomic Molecular and Optical Physics, 2001. 34(9), L281-L288.

41. Cumming, J. B. and Kebarle, P. Summary of gas-phase acidity measurements involving acids AH. Entropy changes in proton-transfer reactions involving negative ions. Bond-dissociation energies D(A-H) and electron affinities EA(A). Canadian Journal of Chemistry-Revue Canadienne De Chimie, 1978. 56(1), 1-9.

42. Martin, J. D. D. and Hepburn, J. W. Determination of bond dissociation energies by threshold ion-pair production spectroscopy: An improved D-0(HCl). Journal of Chemical Physics, 1998. 109(19), 8139-8142.

43. Cai, Y. and Cole, R. B. Stabilization of anionic adducts in negative ion electrospray mass spectrometry. Analytical Chemistry, 2002. 74(5), 985-991.

44. Smith, J. R.; Kim, J. B., and Lineberger, W. C. High-resolution threshold photodetachment spectroscopy of OH^-. Physical Review A, 1997. 55(3), 2036-2043.

45. Squires, R. R. Gas-phase thermochemical properties of the bicarbonate and bisulfite ions. International Journal of Mass Spectrometry and Ion Processes, 1992. 117(1-3), 565-600.

46. Cole, R. B. and Rannulu, N. S. Regioselective anion attachment leading to regiospecific decompositions of bifunctional steroids in negative ion electrospray tandem mass spectrometry. Rapid Communications in Mass Spectrometry, 2011. 25(4), 558-562.

47. Rannulu, N. S. and Cole, R. B. Novel fragmentation pathways of anionic adducts of steroids formed by electrospray anion attachment involving regioselective attachment, regiospecific decompositions, charge-induced pathways, and ion–dipole complex

intermediates. Journal of the American Society for Mass Spectrometry, 2012. 23(9), 1558-1568.

48. Nee, M. J.; Osterwalder, A.; Zhou, J., and Neumark, D. M. Slow electron velocity-map imaging photoelectron spectra of the methoxide anion. Journal of Chemical Physics, 2006. 125(1).

49. Osborn, D. L.; Leahy, D. J.; Kim, E. H.; de Beer, E., and Neumark, D. M. Photoelectron spectroscopy of CH_3O^- and CD_3O^-. Chemical Physics Letters, 1998. 292(4-6), 651-655.

50. Girod, M.; Moyano, E.; Campbell, D. I., and Cooks, R. G. Accelerated bimolecular reactions in microdroplets studied by desorption electrospray ionization mass spectrometry. Chemical Science, 2011. 2(3), 501-510.

51. Kumar, P. P.; Kalinichev, A. G., and Kirkpatrick, R. J. Dissociation of carbonic acid: Gas phase energetics and mechanism from ab initio metadynamics simulations. Journal of Chemical Physics, 2007. 126(20).

Tables

Table 1 Spectrum lists from the CID spectra of the $[M - H + NaF]^-$ ions of 18:1, 18:2, 20:4 and 20:5. Only product ions of greater than 1% relative abundance (RA) are listed; with the exception of the $[M - 2H + Na]^-$ ion from the 18:1-sodium fluoride complex at *m/z* 303. The precursor ion is underlined in each column while (1) and (2) refer to the $[M - H]^-$ and $[M - 2H + Na]^-$ product ions, respectively.

18:1		18:2		20:4		20:5	
m/z	RA%	*m/z*	RA%	*m/z*	RA%	*m/z*	RA%
281.3 (1)	100	279.3 (1)	100	303.3 (1)	16.9	201.2	1.8
303.3 (2)	0.06	301.3 (2)	66.7	325.3 (2)	100	301.3 (1)	8.4
<u>323.3</u>	1.6	<u>321.3</u>	1.8	<u>345.3</u>	9.6	319.3	1.0
						321.3	2.2
						323.3 (2)	100
						<u>343.3</u>	9.4

Table 2 Abundances of the $[M - 2H + Na]^-$ ion normalized to total product ion abundance (*i.e.*, $[M - 2H + Na]^-$ ion abundance/total product ion abundance %) and $[M - 2H + Na]^-/[M - H]^-$ branching ratios calculated from CID spectra for the fatty acid-sodium fluoride complexes of 18:0, 18:1, 18:2, 20:3, 20:3, 20:4, 20:5 and 22:6.

NaF complexes with fatty acids containing 0-6 double bonds							
Fatty acid	18:0	18:1	18:2	20:3	20:4	20:5	22:6
$\frac{[M-2H+Na]^-}{\sum \text{product ions}}\%$	0.031	0.064	39.7	79.5	83.2	84.2	87.5
$\frac{[M-2H+Na]^-}{[M-H]^-}$	$4.7\text{x}10^{-4}$	$6.4\text{x}10^{-4}$	$6.7\text{x}10^{-1}$	4.1	5.9	11.8	46.4

Table 3 Abundances of the $[M - 2H + Na]^-$ ion normalized to total product ion abundance (*i.e.*, $[M - 2H + Na]^-$ ion abundance/total product ion abundance %) and $[M - 2H + Na]^-/[M - H]^-$ branching ratios for the $[M - H + NaX]^-$ ions of 20:3; where X = F^-, Cl^-, OAc^- and $[M - H]^-$. Gas-phase basicities: F^- = 1530 kJ/mol [39, 40]; Cl^- = 1373 kJ/mol [39, 42]; OAc^- = 1429 kJ/mol [39, 41].

NaX complexes with 20:3		
NaF	$\frac{[M-2H+Na]^-}{\sum \text{product ions}}\%$	79.5
	$\frac{[M-2H+Na]^-}{[M-H]^-}$	4.1
NaCl	$\frac{[M-2H+Na]^-}{\sum \text{product ions}}\%$	0.047
	$\frac{[M-2H+Na]^-}{[M-H]^-}$	4.9×10^{-4}
NaOAc	$\frac{[M-2H+Na]^-}{\sum \text{product ions}}\%$	0.17
	$\frac{[M-2H+Na]^-}{[M-H]^-}$	1.8×10^{-3}
Na(20:3-H)	$\frac{[M-2H+Na]^-}{\sum \text{product ions}}\%$	0.19
	$\frac{[M-2H+Na]^-}{[M-H]^-}$	2.0×10^{-3}

Table 4 Ion abundances from low-mass negative ion ESI mass spectra of the following solutions: methanol/water (4:1 v/v); methanol/water (4:1 v/v) with 200 μM NaOH; methanol/water (4:1 v/v) with 200 μM $NaHCO_3$; and methanol/water (4:1 v/v) with 200 μM NaF. ESI mass spectra were recorded under identical conditions and the mass spectrometer was optimized for the detection of methoxide.

	m/z 17 (^-OH)	*m/z* 19 (F^-)	*m/z* 31 ($^-OCH_3$)	*m/z* 61 (HCO_3^-)
Methanol/water (4:1 v/v)	4.28×10^{-2}	2.07×10^{-1}	1.16×10^{2}	4.46×10^{-1}
Methanol/water (4:1 v/v) with 200 μM NaOH	4.71×10^{0}	5.07×10^{0}	1.20×10^{4}	5.28×10^{1}
Methanol/water (4:1 v/v) with 200 μM $NaHCO_3$	4.85×10^{0}	2.23×10^{0}	1.24×10^{4}	5.10×10^{1}
Methanol/water (4:1 v/v) with 200 μM NaF	2.01×10^{0}	5.43×10^{2}	3.40×10^{3}	5.36×10^{1}

Figure and Scheme legends

Figure 1 a) Negative ion ESI mass spectrum of 20:3 with 100 μM NaF. b) CID spectrum of the $[M - H + NaF]^-$ ion of 20:3 at *m/z* 347 from spectrum (a).

Figure 2 Negative ion CID spectra for the $[M - H + NaF]^-$ ions of a) 18:0 at *m/z* 325 and b) 22:6 at *m/z* 369. c) CID spectrum of the *m/z* 349 ion from spectrum (b) acquired in an MS^3 experiment. The *m/z* 349 ion is the $[M - 2H + Na]^-$ ion of 22:6 and is formed via the neutral loss of HF from the *m/z* 369 precursor ion. Fatty acid-sodium fluoride complexes were formed by electrospray ionization of the fatty acids with 100 μM NaF. The *m/z* 183 product ion in spectrum (a) potentially originates from contamination with isobaric C_{12} linear alkylbenzene sulfonates.

Figure 3 Negative ion ESI mass spectra of 3 μM 22:6 in methanol/water/acetonitrile (79:20:1 by volume) with a) 200 μM NaOH, b) 200 μM $NaHCO_3$ and c) no added sodium salt. d) CID spectrum of the [M - 2H + Na] ion at *m/z* 349 from spectrum (a). Gas-phase basicities: HCO_3^- = 1458 kJ/mol [45]; ^-OH = 1606 kJ/mol [39, 44].

Figure 4 Potential energy diagrams for the formation and dissociation of 9:2 complexed with a) NaF and b) NaOH. Energies in kcal/mol are calculated at the M06-2X/6-31+G(d) level and include unscaled zero-point corrections. For the formation of $[M - 2H + Na]^-$ ions, energies and structures provided are for deprotonation at the (i) α-position and (ii) *bis*-allylic position. The site of deprotonation is indicated with an * symbol on both $[M - 2H + Na]^-$ ion structures.

Scheme 1 Proposed mechanism for the formation of the $[M - 2H + Na]^-$ ion of 20:3 via HF neutral loss from the fatty acid-sodium fluoride complex. In this mechanism, proton transfer

occurs from a *bis*-allylic position to the fluoride anion resulting in the neutral loss of HF and formation of a resonance-stabilized carbanion. Note that deprotonation could occur at either *bis*-allylic position leading to two possible isomeric $[M - 2H + Na]^-$ ions for 20:3.

Figure 1

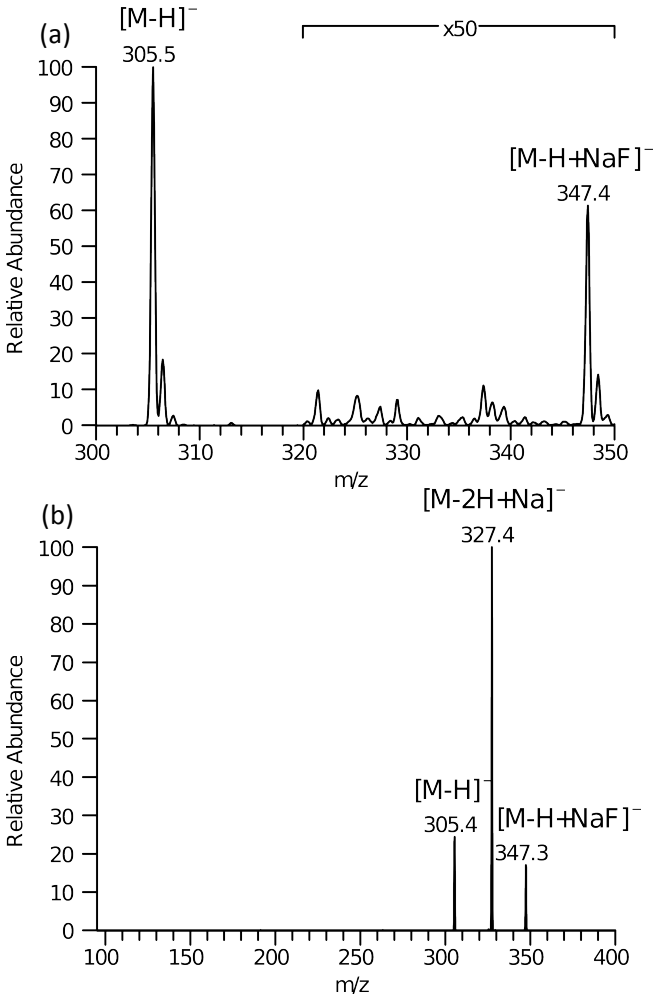
(a)
[M-H]⁻
305.5
x50
[M-H+NaF]⁻
347.4
Relative Abundance
m/z
(b)
[M-2H+Na]⁻
327.4
[M-H]⁻
305.4
[M-H+NaF]⁻
347.3
Relative Abundance
m/z

Figure 2

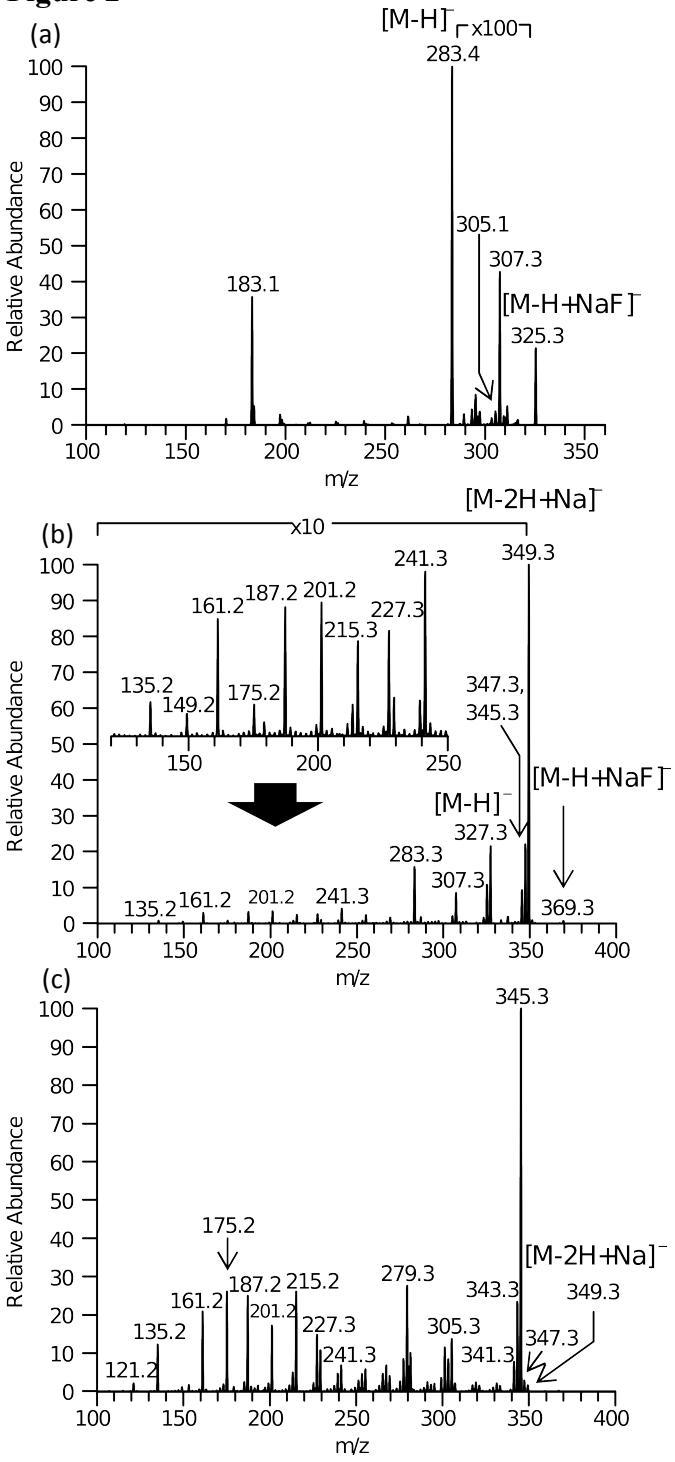
(a)
[M-H]⁻
x100
283.4
305.1
307.3
183.1
[M-H+NaF]⁻
325.3
Relative Abundance
m/z
(b)
x10
[M-2H+Na]⁻
241.3
349.3
161.2
187.2
201.2
227.3
215.3
135.2
149.2
175.2
347.3,
345.3
[M-H+NaF]⁻
[M-H]⁻
327.3
283.3
307.3
135.2
161.2
201.2
241.3
369.3
Relative Abundance
m/z
(c)
345.3
175.2
[M-2H+Na]⁻
279.3
187.2
215.2
343.3
349.3
161.2
201.2
227.3
305.3
135.2
347.3
241.3
341.3
121.2
Relative Abundance
m/z

Figure 3

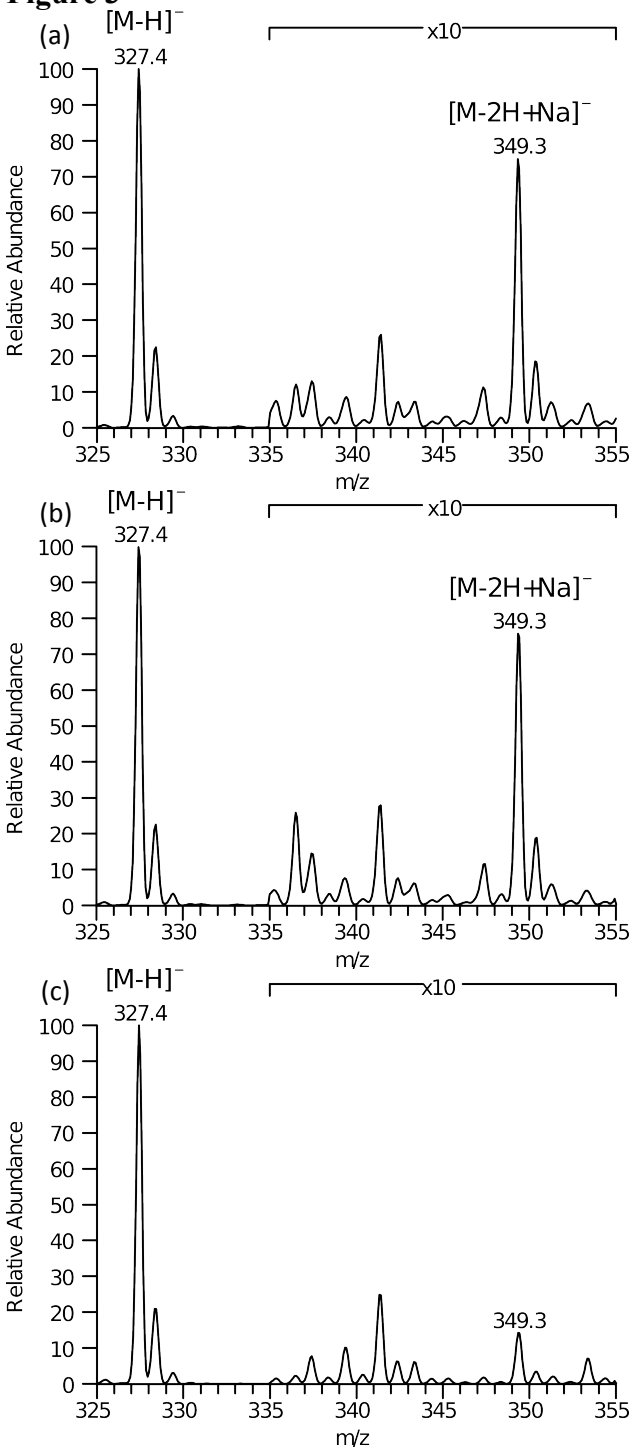
(a)
[M-H]⁻
x10
327.4
[M-2H+Na]⁻
349.3
Relative Abundance
m/z
(b)
[M-H]⁻
x10
327.4
[M-2H+Na]⁻
349.3
Relative Abundance
m/z
(c)
[M-H]⁻
x10
327.4
349.3
Relative Abundance
m/z

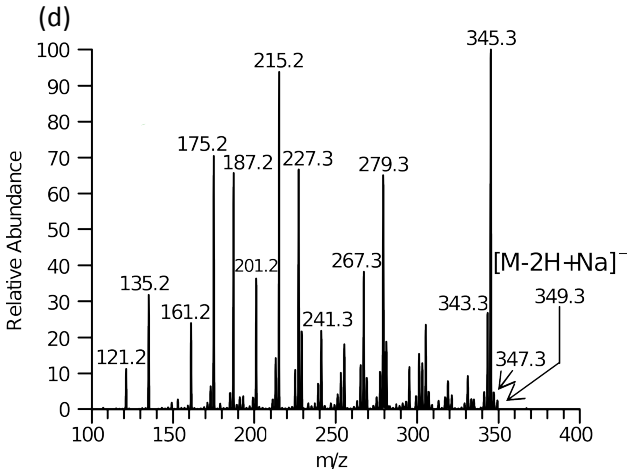
(d)
Relative Abundance
m/z
345.3
215.2
175.2
187.2
227.3
279.3
267.3
[M-2H+Na]⁻
201.2
135.2
161.2
241.3
343.3
349.3
121.2
347.3

Figure 4

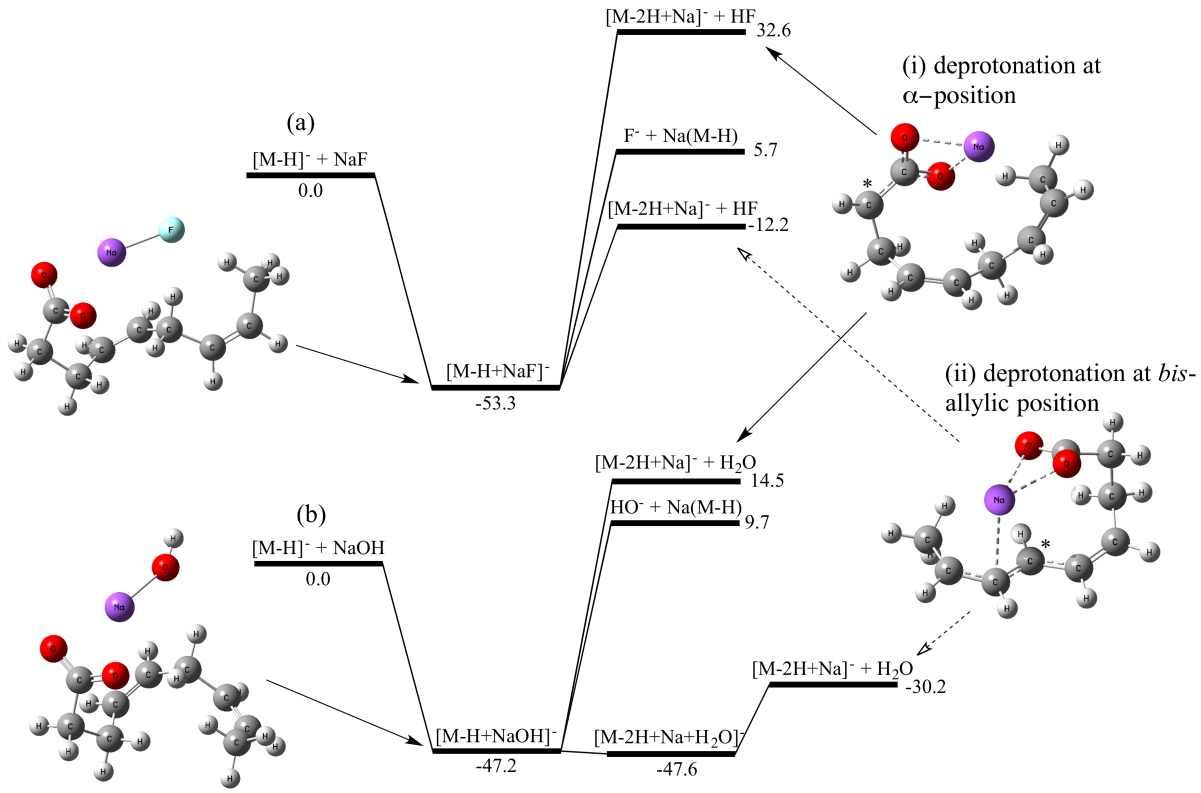
[M-2H+Na]⁻ + HF 32.6
(i) deprotonation at α−position
(a)
[M-H]⁻ + NaF
0.0
F⁻ + Na(M-H) 5.7
[M-2H+Na]⁻ + HF -12.2
[M-H+NaF]⁻
-53.3
(ii) deprotonation at bis-allylic position
[M-2H+Na]⁻ + H2O 14.5
(b)
HO⁻ + Na(M-H) 9.7
[M-H]⁻ + NaOH
0.0
[M-2H+Na]⁻ + H2O -30.2
[M-H+NaOH]⁻
-47.2
[M-2H+Na+H2O]⁻
-47.6

Scheme 1